Modelling and control of a bidirectional rotors X4-flyer

Selima Bennaceur, Naoufel Azouz, Azgal Abichou, Madeleine Pascal

Modelling and control of a bidirectional rotors X4 - flyer

Selima BENNACEUR, Naoufel AZOUZ*, Azgal ABICHOU**, Madeleine PASCAL**

**Informatics, Integrative Biology and Complex Systems,*
40 Rue de Pelvoux, 91020 Evry Cedex, France (e-mail: azouz@iup.univ-evry.fr)
***Ecole Polytechnique de Tunisie B.P. 743 - 2078 La Marsa, Tunisie*

Abstract: This paper presents in the first part the conception and construction of a mini 4 rotors helicopter for indoor and outdoor applications. The proposed UAV, named XSF, has a very manoeuvrable platform and is indicated to work in inaccessible spaces such as performing inspection tasks under bridges as well as inside pipes or tanks. Its main advantage with respect to classical 4 rotors helicopters is the ability of flipping two motors in order to obtain two more control inputs. This feature allows the XSF to have a better horizontal displacement or to create a yaw movement without translation. In the second part, we present a stabilization strategy around a position of equilibrium. The model is highly nonlinear, we use a methodology based on the linearization. The dynamic of the system involves six control inputs which will be computed to stabilize the engine with regard to external perturbations.

Keywords: Unmanned aerial vehicles, robot modeling, stabilization.

1. INTRODUCTION

The recent popularity of the Unmanned Aerial Vehicles (UAV), introduced a need for exploring new civil tasks such as search and rescue, surveillance and inspection. For this purpose, we discuss in this paper the design, modelling and control of a mini-Quadrotor helicopter.

Current literature in the area of design of Quadrotor helicopters focuses on the development of indoor prototypes; see [1-4]. The design proposed is illustrated by very light systems with fixed-rotors. Many groups have seen significant success in developing autonomous quadrotor vehicles [5-11]. However, the main problem associated with this concept is the evident instability of these prototypes in front of atmospheric perturbations especially when manoeuvring.

We propose in this study a suitable design of a quadrotor for outdoor applications with oriented rotors and large energetic autonomy. It is capable of avoiding obstacles, it has an embedded algorithm of stabilization, and it is able to execute an automatic take-off and landing. This UAV can eventually be used by the foot soldiers to explore hostile villages.

Another aspect of the design concerns the automatic control. The oriented rotors give more controllability. On the other hand the control design should combine precision, simplicity and robustness to be easily implemented on board the experimental vehicle.

In this paper we use eulerian parameters. The control strategy is based on the linearization of the local equation. This strategy seems adequate for outdoor applications. Other strategies were presented in the literature. Vision aided control was investigated in [6,9,11].

2. DESIGN AND FABRICATION

The XSF is a quadrirotor of 0.68 m x 0.68 m of total size. It is designed in a cross form and made of carbon fibre. Each tip of the cross has a rotor including an electric brushless motor, a speed controller and a two-blade propeller. In the middle we find a central body enclosing electronics, namely Inertial Measurement Unit, onboard processor ARM 7, a GPS, a radio transmitter, a camera and ultrasound sensors, as well as the 14.8V LI-POLY batteries.

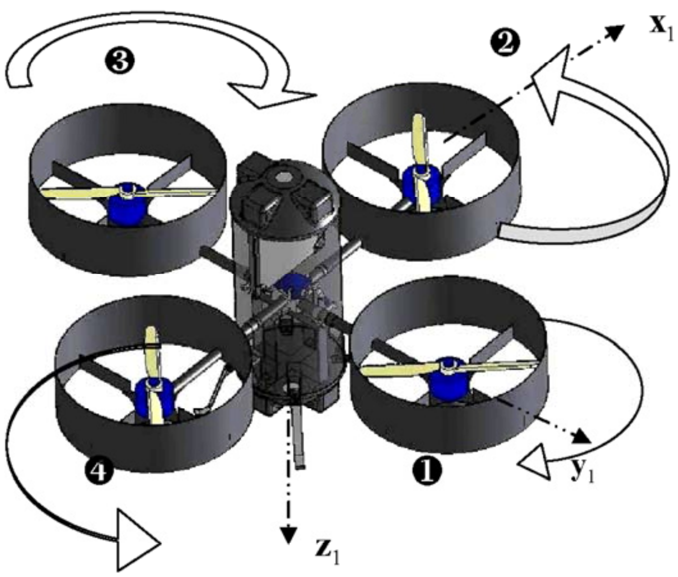

Fig. 1. Representation of the XSF (ducted fan variation).

The operating principle of the XSF can be presented thus:

Rotors ❶ and ❸ turn clockwise, and the rotors ❷ and ❹ turn in the opposite direction to maintain the total equilibrium in yaw motion. Assuming the equilibrium of the angular velocities of all rotors, the UAV is either in stationary position, or moving vertically (ascending or descending).

A characteristic of the XSF compared to the existing quadrotors, is the swivelling of the supports of the motors ❶ and ❸ around the pitching axis $\mathbf{y}_1$. This permits an adequate horizontal flight and a suitable cornering.

3. DYNAMIC MODEL

3.1. *Kinematics*

The XSF is modelled in first approximation as a rigid flying object. We use here an eulerian approach. A lagrangian approach can be seen in [12], [5].
The motion of the UAV is described by the following parameters:
$\eta_1=[x_1, y_1, z_1]^T$: Vector position of the origin expressed in the fixed reference frame,
$\eta_2=[\phi, \theta, \psi]^T$: Vector orientation of the local reference frame and given by the Euler angles,
$\nu_1=[u,v,w]^T$: Velocity Vector compared to the fixed frame expressed in the local frame,
$\nu_2=[p, q, r]^T$: Vector of angular velocities compared to the fixed frame expressed in the local frame, and m is the mass of the UAV.
Commonly in aeronautics, a parameterization in yaw ψ, pitch θ and roll ϕ is used to describe the orientation of the UAV.
The whole transformation between the fixed frame and the local reference frame is the combination of elementary matrices of rotation around the three axes $\vec{z}$, $\vec{y}_1$, and $\vec{x}_2$, and is denoted by J_1 .
We denote by: $c\theta = \cos\theta \quad ; s\phi = \sin\phi$
Using the rotation matrix $J_1(\eta_2)$, the expression of the linear speed in the reference frame R_0 is given by:

$$\dot{\eta}_1 = J_1(\eta_2).\nu_1 \tag{1}$$

On the other hand, the angular speed of the UAV ν_2 is the combination of the angular speeds around the three axes of yaw, pitch and roll. It can be written related to $\dot{\eta}_2$ as:

$$\nu_2 = \begin{pmatrix} p \\ q \\ r \end{pmatrix} = \begin{pmatrix} 1 & 0 & -s\theta \\ 0 & c\phi & s\phi c\theta \\ 0 & -s\phi & c\phi c\theta \end{pmatrix} . \begin{pmatrix} \dot{\phi} \\ \dot{\theta} \\ \dot{\psi} \end{pmatrix} \tag{2}$$

or :

$$\dot{\eta}_2 = J_2(\eta_2).\nu_2 \tag{3}$$

It is noticed that the parameterization by the Euler angles have a singularity in $\theta = \frac{\pi}{2} + k\pi$.
The global kinematics equation is then:

$$\dot{\eta} = \begin{pmatrix} J_1(\eta_2) & 0 \\ 0 & J_2(\eta_2) \end{pmatrix} \begin{pmatrix} \nu_1 \\ \nu_2 \end{pmatrix} \tag{4}$$

The dynamical system of the XSF expressed with the Euler variables becomes (see [13]):

$$\begin{pmatrix} m_{TT} & 0 \\ 0 & I_{RR} \end{pmatrix} \begin{pmatrix} \dot{\nu}_1 \\ \dot{\nu}_2 \end{pmatrix} = \begin{pmatrix} Z_T - m_{TT}(\nu_2 \wedge \nu_1) \\ Z_R - \nu_2 \wedge (I_{RR}\nu_2) \end{pmatrix} \tag{5}$$

Or in compact form:

$$M_E \dot{\nu} = \overline{Z} + Q_G \tag{6}$$

M_E is the constant mass matrix, and I_{RR} is the inertia tensor.
$\dot{\nu} = \begin{pmatrix} \dot{\nu}_1 \\ \dot{\nu}_2 \end{pmatrix}$, $\overline{Z} = \begin{pmatrix} Z_T \\ Z_R \end{pmatrix}$, are respectively the acceleration vector and the vector of generalized external forces and torques, and finally $Q_G = \begin{pmatrix} -m_{TT}(\nu_2 \wedge \nu_1) \\ -\nu_2 \wedge (I_{RR}\nu_2) \end{pmatrix}$ is a vector containing the gyroscopic and Coriolis forces.
Taking into account that the plan x-z and y-z are plans of symmetry of the XSF, we conclude that the inertia products I_{xy}, I_{xz} and I_{yz} are null.
The gyroscopic effects of the rotating elements (rotors) are also introduced in the model as it follows:
Let us denote $\overline{\overline{I}}_R\, \boldsymbol{\omega}_i$ the kinetic moment of the rotor (i). where $\boldsymbol{\omega}_i$ is the rotational velocity vector of the rotor (i), I_R is the inertia moment of the rotating elements in the rotors.
An additional gyroscopic effect $\overline{\overline{I}}_R . \sum_{i=1}^{4} \omega_i . \wedge \nu_2$ is then included in Z_R.

3.2. *Aerodynamic forces and torques*

In this part, we define the characteristics of the aerodynamic forces and torques issued from the blade theory.

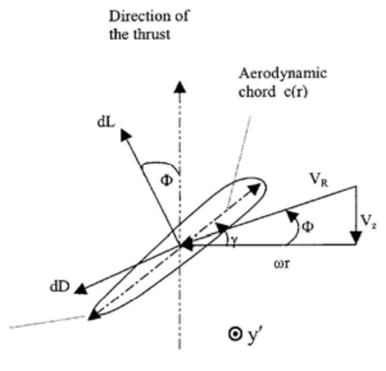

Fig. 2. Description of forces applied on the blade

The blade behaves as a rotating wing. Each element of the blade dr is in contact with the airflow. The local dynamic pressure at the blade element is: $q = \frac{1}{2}\rho(\omega r)^2$.

Each elementary section of the blade of width dr creates a lift dL such as [14]:

$$dL = \frac{1}{2}\rho\,(\omega r)^2\, C_{L\alpha}.c.\alpha.dr \tag{7}$$

Where ρ is the air density, $C_{L\alpha}$ represents a non-dimensional coefficient of the gradient of lift. The angle of attack a is such $\alpha = \gamma - \Phi$.

γ is the geometric pitch of the blade, Φ the local inflow angle, and finally c is the aerodynamic chord that we assume constant here.

The integration of this elementary lift all over the blade gives this relation :

$$\overline{F} = k_T\,\omega^2 \tag{8}$$

The drag is defined similarly to the lift, and produces a torque defined such as :

$$M_D = k_M\,\omega^2 \tag{9}$$

The compensation of this torque in the centre of gravity is established thanks to the use of contrarotating rotors 1-3 and 2-4. Recalling that by assumption we have $w_1 < 0$ and $w_3 < 0$. These last two rotors having propellers with reversed pitch.

3.3. *Swivelling of the rotors ❶ and ❸*

To allow the horizontal displacement of the XSF without banking, we give the driving supports ❶ and ❸ an additional degree of freedom. It concerns the rotation around the axis $\vec{y}$. We denote by β this swing angle. The two driving supports can either swivel in the same direction to create a horizontal component propelling the XSF in translation, or swivel in opposite directions to create a yaw without translation.

In addition, we call E the centre of the brace, intersection of the four supports, such as $\|EG\| = u_G$. We assume that the forces F_1 and F_3 are applied on the support edges ❶ and❸.

We must note that the swivelling of these rotors can destroy the aerodynamic equilibrium in yaw, and can create a rolling torque. The controller should be robust enough to take into account this particularity.

3.4. *Complete Model*

According to the preceding relations, the equation (6) could be written in an expanded form as:

$$\begin{cases} m\dot{u} = m(-q.w + r.v - g.s\theta) - k_T(\omega_1^2.s\beta_1 + \omega_3^2.s\beta_3) \\ m\dot{v} = m(-r.u + p.w + g.s\phi.c\theta) \\ m\dot{w} = -k_T(\omega_1^2\, c\beta_1 + \omega_2^2 + \omega_3^2\, c\beta_3 + \omega_4^2) \\ \qquad + m(-p.v + q.u + g.c\phi.c\theta) \end{cases} \tag{10}$$

Where g is the acceleration of the gravity, and :

$$\begin{cases} I_{xx}\dot{p} = l_b k_T(\omega_1^2.c\beta_1 - \omega_3^2.c\beta_3) - (I_{zz} - I_{yy})r.q \\ \quad - q\,I_R(\omega_1.c\beta_1 + \omega_2 + \omega_3.c\beta_3 + \omega_4) \\ \quad + k_M(-\omega_1^2.s\beta_1 - \omega_3^2.s\beta_3) \\ I_{yy}\dot{q} = l_b k_T(\omega_2^2 - \omega_4^2) - r\,I_R(\omega_1.s\beta_1 + \omega_3.s\beta_3) - (I_{xx} - I_{zz})p.r + \\ \quad u_G.k_T(\omega_1^2.s\beta_1 + \omega_3^2.s\beta_3) + \; pI_R(\omega_1.c\beta_1 + \omega_2 + \omega_3.c\beta_3 + \omega_4) \\ I_{zz}\dot{r} = -l_b k_T(\omega_1^2.s\beta_1 - \omega_3^2.s\beta_3) - (I_{yy} - I_{xx})p.q \\ \quad + q\,I_R(\omega_1.s\beta_1 + \omega_3.s\beta_3) + k_M(\omega_1^2.c\beta_1 - \omega_2^2 + \omega_3^2.c\beta_3 - \omega_4^2) \end{cases} \tag{11}$$

The global velocities expressed in the fixed-earth frame can be found by these relations:

$$\begin{cases} \dot{x}_o = c\theta.c\psi.u + (s\phi.s\theta.c\psi - c\phi s\psi)\,v + (c\phi.s\theta.c\psi + s\phi.s\psi)\,w \\ \dot{y}_o = c\theta.s\psi.u + (s\phi.s\theta.s\psi + c\phi.c\psi)\,v + (c\phi.s\theta.s\psi - s\phi.c\psi)\,w \\ \dot{z}_o = -s\theta.u + s\phi.c\theta.v + c\phi.c\theta.w \end{cases} \tag{12}$$

If we do not consider the effect of the atmospheric wind, the equations of motion are summarised in the equations (4), (10), (11) and (12).

4. CONTROL STRATEGY

The XSF is controlled by varying the rotor speeds, thereby changing the lift forces, and by inclining the oriented rotors. Although it has six input forces (four generated by the main motors, and two by the servomotors), it is an under-actuated dynamic vehicle. This system is highly manoeuvrable, enabling vertical take-off and landing, as well as flying into almost inaccessible areas. The disadvantages are the increased helicopter weight and increased energy consumption due to the extra motors. Since it is controlled with rotor speed changes, it is more suitable to electric motors.

In this part we will establish a strategy to stabilize the XSF. In order to simplify the expressions, we use some intermediate notations, thus we note:

$$\begin{cases} u_1 = -k_T(\omega_1^2.s\beta_1 + \omega_3^2.s\beta_3) \\ u_2 = -k_T(\omega_1^2.c\beta_1 + \omega_2^2 + \omega_3^2.c\beta_3 + \omega_4^2) \\ u_3 = l_b k_T(\omega_1^2.c\beta_1 - \omega_3^2.c\beta_3) + \\ \qquad k_M(-\omega_1^2.s\beta_1 - \omega_3^2.s\beta_3) \\ u_4 = l_b k_T(\omega_2^2 - \omega_4^2) + u_G k_T(\omega_1^2.s\beta_1 + \omega_3^2.s\beta_3) \\ u_5 = -l_b k_T(\omega_1^2.s\beta_1 - \omega_3^2.s\beta_3) \\ u_6 = k_M(\omega_1^2.c\beta_1 - \omega_2^2 + \omega_3^2.c\beta_3 - \omega_4^2) \end{cases} \tag{13}$$

β_1 and β_3 are the two internal degrees of freedom of rotor ❶ and❸, respectively.

We denote: $f_1 = k_T\omega_1^2$; $f_2 = k_T\omega_2^2$; $f_3 = k_T\omega_3^2$; and $f_4 = k_T\omega_4^2$

REMARK:
As shown the equivalent system of control presents six inputs:

$$U = \begin{pmatrix} u_1 & u_2 & u_3 & u_4 & u_5 & u_6 \end{pmatrix}^T.$$

While the rotor force-inputs are of six orders :

$$F = \begin{pmatrix} f_1 & f_2 & f_3 & f_4 & s\beta_1 & s\beta_3 \end{pmatrix}^T.$$

Thus the transformation $U \rightarrow F$ is given by $U = A\,F$.

The system is nonlinear. The problem will then be solved numerically by an implicit process.
Considering in this part a small deviation around a position of equilibrium. As our model is local and Eulerian, we will use the theory of small perturbations. This simplified theory gives good results, specially in the stability analysis of the equilibrium states and the response to commands.

4.1. Linearization of equations
This process begins by decomposing the motion between the equilibrium state and the deviation from this state. The idea is to stabilize the XSF around a position of equilibrium defined as follows:

$$u_d = v_d = w_d = p_d = q_d = r_d = \theta_d = \phi_d = 0 \qquad (14)$$

Where the label d is used for the desired parameters.
Under these conditions, and when neglecting the variation of the quadratic terms, and when linearizing the trigonometric expressions, the dynamic equations become:

$$\begin{cases} m\Delta\dot{u} = -mg\Delta\theta + u_1 \\ m\Delta\dot{v} = -mg\Delta\phi \\ m\Delta\dot{w} = -mg + u_2 \end{cases} \quad \begin{cases} I_{xx}\Delta\dot{p} = u_3 \\ I_{yy}\Delta\dot{q} = u_4 \\ I_{zz}\Delta\dot{r} = u_5 + u_6 \end{cases} \quad \begin{cases} \dot{\varphi} = \Delta p \\ \dot{\theta} = \Delta q \\ \dot{\psi} = \Delta r \end{cases} \qquad (15)$$

Under the desired conditions (21) we will have:

$$\Delta u = u;\ \Delta v = v;\ \Delta w = w;\ \Delta p = p;\ \Delta q = q;\ \Delta r = r$$

$$\Delta\dot{u} = \dot{u};\ \Delta\dot{v} = \dot{v};\ \Delta\dot{w} = \dot{w};\ \Delta\dot{p} = \dot{p};\ \Delta\dot{q} = \dot{q};\ \Delta\dot{r} = \dot{r}$$

and the kinematics part is given by:

$$\Delta p = \dot{\phi}\,;\quad \Delta q = \dot{\theta}\,;\quad \Delta r = \dot{\psi}$$

4.2. presentation of the controller

In this work, the originality is the use of the Eulerian variables. These variables are more realistic, because they correspond to the data given by the embedded sensors. We underline that some degrees of freedom such as roll and pitch are particularly critical for the stabilization of the quadrotor when hovering. A sample blast of wind can destabilize the UAV and leads to the crash. It is then important to stabilize efficiently these two degrees of freedom.
In this study the whole commands are disconnected. The different motions of translation or rotation can be stabilized by linear controllers such as described in tab.1. k_i are positive gains.

Motion	**Relation acceleration/control**	**Control of the speed**	**acceleration**
Translation xx	$m\dot{u} = -m.g.(\theta-\theta_d) + u_1$	$u_1 = -m.k_1(u-u_d) + m.g.(\theta-\theta_d)$	$\dot{u} = -k_1(u-u_d)$
Translation zz	$m\dot{w} = m.g + u_2$	$u_2 = -m.k_2(w-w_d) - m.g$	$\dot{w} = -k_2(w-w_d)$
Roll	$\dot{p} = \frac{1}{I_{xx}}u_3$	$u_3 = -I_{xx}(k_3(p-p_d) - k_4(\varphi-\varphi_d))$	$\dot{p} = -k_3(p-p_d) - k_4(\varphi-\varphi_d)$
pitch	$\dot{q} = \frac{1}{I_{yy}}u_4$	$u_4 = -I_{yy}(k_5(q-q_d) - k_6(\theta-\theta_d))$	$\dot{q} = -k_5(q-q_d) - k_6(\theta-\theta_d)$
yaw	$\dot{r} = \frac{1}{I_{zz}}(u_5+u_6)$	$u_5 = -I_{zz}k_7(r-r_d)$ $u_6 = -I_{zz}k_8(\psi-\psi_d)$	$\dot{r} = -k_7(r-r_d) - k_8(\psi-\psi_d)$

Tab. 1 Stabilization strategy

Finally we input these controls in the complete model, with nonlinear terms such as:

$$
\begin{cases}
\dot{u} = \dfrac{u_1}{m} - g.s\theta - (q.w - r.v) \\
\dot{w} = \dfrac{u_2}{m} + g.c\varphi.c\theta - (p.v - q.u) \\
\dot{p} = \dfrac{1}{I_{xx}} u_3 - \dfrac{(I_{zz} - I_{yy})}{I_{xx}} r.q \\
\quad - q\dfrac{I_R}{I_{xx}}(\omega_1.c\beta_1 + \omega_2 + \omega_3.c\beta_3 + \omega_4) \\
\dot{q} = \dfrac{1}{I_{yy}} u_4 - \dfrac{(I_{xx} - I_{zz})}{I_{yy}} r.p - r\dfrac{I_R}{I_{yy}}(\omega_1.s\beta_1 + \omega_3.s\beta_3) \\
\quad + p\dfrac{I_R}{I_{yy}}(\omega_1.c\beta_1 + \omega_2 + \omega_3.c\beta_3 + \omega_4) \\
\dot{r} = \dfrac{1}{I_{zz}}(u_5 + u_6) - \dfrac{(I_{yy} - I_{xx})}{I_{zz}} q.p + \\
\quad q\dfrac{I_R}{I_{zz}}(\omega_1.s\beta_1 + \omega_3.s\beta_3)
\end{cases} \tag{16}
$$

Note that the UAV state is supposed to be measurable or observable.

4.3. Analysis of the actuators

In this paragraph, we incorporate relations between the propeller forces and the preceding command (u_1-u_6). Recall that the XSF is equipped with four brushless motors. The variation of current permits to adjust the motor angular speed and then the propeller's forces. The angles of orientation β_1 and β_3 insure the translation motion, the Yaw motion, and the cornering.

By using the equation (14), we remark that we have a nonlinear system. So in order to compute the column matrix of the actuators, we built a matrix (A) which connects the six actuators and the commands. This matrix will be computed numerically and actualized at each time in the simulation.

For example at t^{n-1}

$$
\begin{pmatrix} u_1 \\ u_2 \\ u_3 \\ u_4 \\ u_5 \\ u_6 \end{pmatrix} = \underbrace{\begin{pmatrix}
0 & 0 & 0 & 0 & -f_1^{n-1} & -f_3^{n-1} \\
-(1-(s^2\beta_1)^{n-1})^{\frac{1}{2}} & -1 & -(1-(s^2\beta_3)^{n-1})^{\frac{1}{2}} & -1 & 0 & 0 \\
-l_b(1-(s^2\beta_1)^{n-1})^{\frac{1}{2}} & 0 & l_b(1-(s^2\beta_3)^{n-1})^{\frac{1}{2}} & 0 & \frac{-K_M}{K_T} f_1^{n-1} & \frac{K_M}{K_T} f_3^{n-1} \\
0 & l_b & 0 & -l_b & U_G f_1^{n-1} & U_G f_3^{n-1} \\
0 & 0 & 0 & 0 & -l_b f_1^{n-1} & -l_b f_3^{n-1} \\
\frac{-K_M}{K_T}(1-(s^2\beta_1)^{n-1})^{\frac{1}{2}} & \frac{K_M}{K_T} & \frac{-K_M}{K_T}(1-(s^2\beta_3)^{n-1})^{\frac{1}{2}} & \frac{K_M}{K_T} & 0 & 0
\end{pmatrix}}_{A} \begin{pmatrix} f_1 \\ f_2 \\ f_3 \\ f_4 \\ s\beta_1 \\ s\beta_3 \end{pmatrix} \tag{17}
$$

Thus by inverting this matrix (A) we find the generalized column matrix of the actuators.

The previous algorithm is programmed numerically using advanced difference.

5. SIMULATION RESULTS

To demonstrate the usefulness of the procedure proposed before, we stabilize our system in different configurations. Realistic constraints are introduced into the system. This concern namely the maximum force that can be produced by a rotor (this means implicitly the saturation of the motors), and the maximum angle of rotation of the oriented rotors. We show below the efficiency of the algorithm in front of different kinds of perturbations introduced as initial conditions.

We choose identical gains

$$k_1 = k_2 = k_3 = k_4 = k_5 = k_6 = k_7 = k_8 = 10$$

THE ROLLING AND PITCHING MOTION

We introduce here a perturbation combining roll and pitch motions. Those motions are the most critical ones in term of stability. It is then necessary to obtain satisfactory results for this simulation. The numerical results are presented in the following figures:

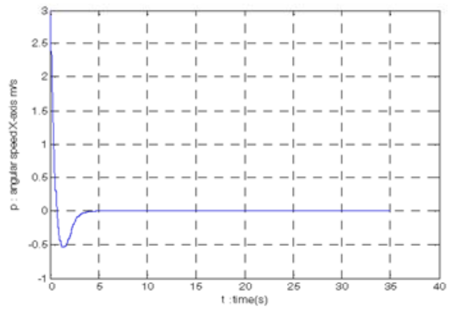

Figure 3- The angular speed around the x-axis.

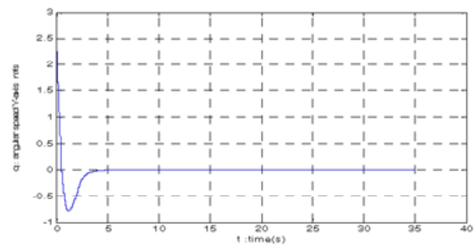

Figure 4- The angular speed around the y-axis.

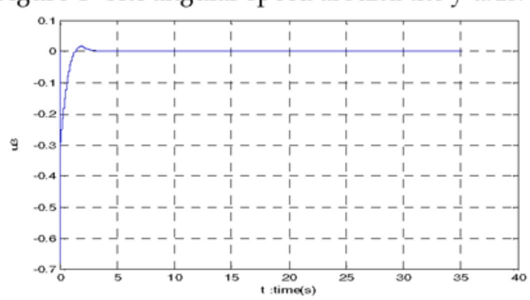

Figure 5- The Control u_3.

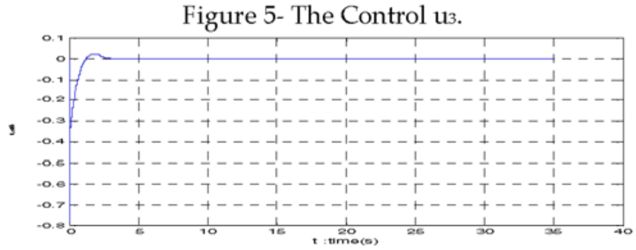

Figure 6- The Control u_4.

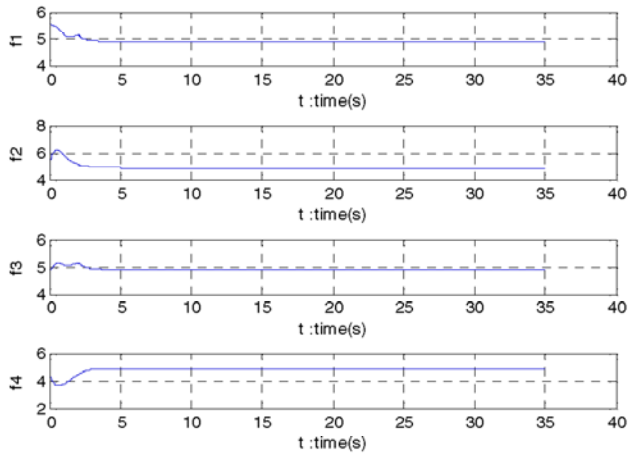

Figure 7- Forces developed by the rotors.

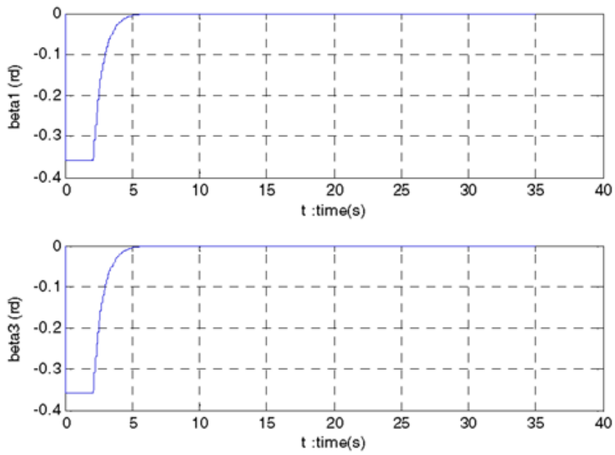

Figure 8- The angles of orientation.

Figures 3-8 show the response of the system in case of coupled perturbations (roll and pitch initial speed). The system is stabilized and reaches a horizontal trim in less than five seconds, proving that the stabilization of the motion is fairly robust. In the figure 3-4, we notice that the rotation speeds of the engine reach the desired speed in 2 seconds and they tend towards zero. However, In figure 7 we can notice that in a transient period the forces f_i reach the maximum value of 6N without exceeding it.

6. CONCLUSION

We have presented the XSF drone, a novel 4 rotors flying robot which presents a new design compared to the classical quadrotor version. This small drone is semi-autonomous and may perform

different tasks of supervision and inspection following high level commands from a remote human operator. We have presented its physical model, its mechanical construction, the embedded electronics and informatics and its control strategy.

For the moment, the proposed drone has only flown on a test bed, and future steps will be flying

tests on outdoors, the coupling of the observer algorithm to the controller, and the human-machine interface in order to close the loop.

REFERENCES

[1] Marti S. (2000). "The zero G eye: Towards a free hovering camera". Technical Report, MIT, Massachusetts, USA.

[2] Sacco, N. "How the Dragan Flyer Flies". www.rctoys.com

[3] Kroo I. and Printz, F. "Mesicopter Project", Stanford University,: http://aero.Stanford.edu/ Mesicopter

[4] Borenstein, J. (2002). "Hoverbot Project", unpublished paper. http://www.valentiniweb.com/piermo/ robotica/doc/Borenstein/paper99.pdf

[5] Castillo P., Dzul A., Lozano R. (2004). "Real-time stabilization and tracking of a four rotor Mini-Rotorcraft". IEEE Transactions on Control Systems Technology, Regular paper, Vol.12, Issue 4, pp. 510-516.

[6] Altug E., Ostrowski J., Mahony R., (2002). "Control of a quadrotor helicopter using visual feedback". Proceedings of the IEEE Int. Conference on Robotics and Automation, ICRA '02, Washington DC, USA.

[7] Guenard N., Hamel T., Eck L. (2006). "Control law for the teleoperation for an UAV known as an X4-flyer", IROS. CHINA.

[8] Hamel, T., Mahony R., Lozano R. and , Ostrowski J.P. (2002). "Dynamic modelling and configuration stabilization for an X4-Flyer", in IFAC 15th Wold Congress Automatic Control.

[9] Romero H., Benosman R, and Lozano R. (2006). " Stabilization and location of a four rotor helicopter applying vision", ACC, 3930-3936, Minneapolis, USA.

[10] Bouabdallah S., Murrieri P., and Siegwart R. (2004). " Design and control of an indoor micro quadrotor", ICRA, New Orleans, USA.

[11] Altug, E. (2003). "Vision based control of unmanned aerial vehicles with applications to an autonomous four rotor helicopter, quadrotor" Ph.D. dissertation, faculties of the university of Pennsylvania.

[12] Beji L., Abichou A., Azouz N. (2006). "Modelling, Motion Planning and Control of the Drones with Revolving Airfoils: an Outline of the XSF". Robot Motion and Control Recent Developments Series: Lecture Notes in Control and Information Sciences , Vol. 335 Kozlowski, Krzysztof (Ed.), ISBN: 1-84628-404-X.

[13] Bennaceur S., Azouz N., Abichou A. (2006). "An Efficient Modeling of Flexible Blimps: Eulerian Approach". Proceedings of the AIAA Guidance, Navigation, and Control Conference. AIAA-2006-6621. Keystone, CO, USA.

[14] Prouty, R. W. (1995). "Helicopter Performance, Stability and Control". Krieger Publishing Company. USA.